

## TiO<sub>2</sub> based surface acoustic wave gas sensor with modified electrode dimensions for enhanced H<sub>2</sub> sensing application

Nimmala Harathi<sup>1</sup>, Argha Sarkar<sup>2,\*</sup>

<sup>1</sup>Nanoelectronics Lab, Department of Electronics & Instrumentation Engineering, Sree Vidyanikethan Engineering College, Tirupati, 517102, India

<sup>2</sup>Electronics and Communication Engineering, Vishnu Institute of Technology, Andhra Pradesh, 534202, India

Received 17 August 2020;

revised 15 September 2020;

accepted 01 October 2020;

available online 03 October 2020

### Abstract

The design and optimization of nanostructure-based surface acoustic wave (SAW) gas sensor is analyzed based on TiO<sub>2</sub> sensing layer and modified electrode dimensions. The sensitivity of the gas sensor depends upon the type of sensing layer used and active surface area obtained by varying the aspect ratio. The performance of the sensor is observed from 0.1ppm to 100ppm concentration of hydrogen gas with respect to output displacement. The displacement of the sensor increases with the increase in concentration. The characteristic of the sensor is also studied by varying input and output interdigital transducers' (IDT) height from 0.05µm to 0.5µm. The nanostructured TiO<sub>2</sub> based sensor has shown increased total displacement and frequency shift of the device resulting enhanced sensitivity. At 0.05 µm IDT height the displacement is found to be a maximum. The operating frequency is considered to be 44 Mhz. Finite Element Modeling (FEM) is used for analysis of the sensor. Simulation is done in software named COMSOL Multiphysics to ensure the enhanced performance of the mechanically engineered surface-based (nanorod) SAW gas sensor.

**Keywords:** COMSOL; IDT; SAW; Sensor Response; TiO<sub>2</sub>.

### How to cite this article

Harathi N., Sarkar A. TiO<sub>2</sub> based surface acoustic wave gas sensor with modified electrode dimensions for enhanced H<sub>2</sub> sensing application. *Int. J. Nano Dimens.*, 2020; 12(1): 83-89.

### INTRODUCTION

Gas Sensors play a vital role in day to day life specially in environmental monitoring, and mining field. Development in vehicular traffic and high industrialization lead to production of many gases [1]. The concentration of gases should lie in perishable limits while in to the environment or in the mining. So, it is necessary to detect the gas even if the concentration of the gas is very low. Surface acoustic wave (SAW) based gas sensors have been widely used in different fields (detection of physical, chemical and biological chemical quantities) and will endure to be of abundant significance in the anticipatable future.

Besides, interesting sensing technique, the low insertion loss and high sensitivity have made its application more prominent in the field of sensor technology. The sensing layer plays a major role in the SAW sensor to enhance the sensitivity [2].

A few works have been reported so far based on SAW technology. Shahrzad Arabshahi *et al.* [3] have constructed a SAW based NO<sub>2</sub> gas sensor to sense 100ppm of gas with ZnO as sensing Layer at room temperature. Sai Pavan Rajesh. Valluru *et al.* [4] have figured a 3D model saw sensor using Focused Inter Digital Transducer Design which is reliable in operation and helps in energy optimization. Sarkar *et al.* have [5] simulated a saw based ethylene gas sensor for testing the maturity

\* Corresponding Author Email: [argha15@gmail.com](mailto:argha15@gmail.com)

level of fruit using ZnO as sensing layer. S. Ippolito *et al.* [6] have designed a layered SAW sensor which will respond to ethylene gas vapours and humidity. A. Sarkar *et al.* [7] have reported about the responsivity optimization of methane gas sensor using SAW technology. From the reported works it is understood that the detection or sensing of physical and chemical quantities using SAW based devices are having potential applications. The SAWs in consideration of gas sensor enhances the sensing mechanism with higher sensitivity because of the fundamental technique of interaction between the acoustic propagation, which results in the sensor response, comprises several linear and non linear properties of the propagation medium allied to elastic stiffness, mass density, behaviour of piezoelectric materials, and electric-dielectric properties. Moreover, SAWs are turned out to be highly sensitive to surface perturbations of the propagation medium because the acoustic energy is constricted to a thin near-surface part of the substrate.

Herein, a SAW-based H<sub>2</sub> gas sensor is simulated to monitor its performance. A sensing layer, an IDT, and a piezoelectric substrate are the major three constituents in a SAW sensor. The IDT dimension is one of the important parameters to determine the synchronous frequency of the acoustic sensor. Different IDT dimensions are considered to transform an electrical pulse into an acoustic wave by engendering a mechanical force via the piezoelectric effect [8-11] and thus to compare the efficiency in terms of IDT dimensions. TiO<sub>2</sub> is considered as sensing layer and compared their sensing performance by keeping the active layer between the input IDT and the output IDT to interact with target analytes. An investigation is made by optimizing wave properties, importantly frequency shift and the total displacement.

**MATERIALS AND METHODS**

The working of SAW based gas sensor relay on propagation of surface acoustic wave. The propagation of surface wave in turn depends on nature off sensing layer and properties piezoelectric substrate. The SAW based gas sensor uses a piezoelectric substrate upon which a sensing layer is placed. The sensing layer contains input and output IDT [12-17]. The input and output IDTs are enabled with alternating potentials. When a sinusoidal signal is applied to the input IDT, the alternating potential at the IDT develops stress

on the piezoelectric substrate which results in production of surface acoustic wave [8]. This surface acoustic wave propagates over the surface of the sensing layer and gets altered by the nature of sensing layer. The arrival of the acoustic at the output IDT gets altered by the alternating potential of IDT and gets converted to electric potential. Ultimately, the input IDT converts electrical signal into a surface acoustic wave signal and output IDT converts surface acoustic wave into an electrical signal [18-19]. The surface acoustic wave is defined by its velocity of propagation which results in change in frequency and its amplitude which results in change of displacement. The generated SAW propagates over the surface of sensing layer and gets altered by the nature of sensing layer and by the type of gas deposited. It causes a change in frequency and displacement of the saw wave [20-23].

The sensor mainly contains a piezoelectric substrate over which the sensing layer is placed; this sensing layer is wrapped with input and output IDTs. The piezoelectric substrate possesses the piezoelectric property which converts mechanical energy into electrical energy and electrical energy into mechanical energy [9]. Among many piezoelectric materials available the most suited for this application is lithium niobate (LiNbO<sub>3</sub>) which is having highest electromechanical coupling coefficient and it may optimize the sensor performance [24-26]. The piezoelectric, elastic constants and permeability constants are expressed in the equation 1, 2 and 3 respectively. The corresponding valves of constants are shown in valves shown in Table1.

$$C = \begin{pmatrix} c_1 & c_2 & c_3 & c_4 & 0 & 0 \\ c_2 & c_1 & c_3 & -c_4 & 0 & 0 \\ c_3 & c_3 & c_3 & 0 & 0 & 0 \\ c_4 & -c_4 & 0 & c_4 & 0 & 0 \\ 0 & 0 & 0 & 0 & c_4 & c_4 \\ 0 & 0 & 0 & 0 & c_4 & (c_1 - c_2)/2 \end{pmatrix} \tag{1}$$

$$e = \begin{pmatrix} 0 & 0 & 0 & 0 & e_5 & -e_2 \\ -e_2 & e_2 & 0 & e_5 & 0 & 0 \\ e_3 & e_3 & e_3 & 0 & 0 & 0 \end{pmatrix} \tag{2}$$

$$\epsilon = \begin{pmatrix} \epsilon_1 & 0 & 0 \\ 0 & \epsilon_1 & 0 \\ 0 & 0 & \epsilon_3 \end{pmatrix} \tag{3}$$

In the piezoelectric material, the acoustic

Table 1. Piezoelectric material constants.

Name of the parameter	Constant	Value of the constant
Elastic constants	c11	2.02×10 <sup>11</sup> N/m <sup>3</sup>
	c12	0.573
	c13	0.752
	c14	0.085
	c33	2.424
	c44	0.595
Piezoelectric constants	e15	3.7 C/ m <sup>3</sup>
	e22	2.5
	e31	0.23
	e33	1.33
Permeability constants	ε11	85.2
	ε13	28.7
Density	ρ	47000kg/m <sup>3</sup>

wave propagates which is a function of stress and electric displacement. The stress experienced in turn depends on elasticity matrix, piezoelectric coupling constant and electric field intensity. The electrical displacement depends on electric field intensity and permeability of the piezoelectric material. The stress produced in the acoustic wave is expressed as equation 4 and the electrical displacement is calculated from equation 5 [10-11].

$$T = cS - eE \tag{4}$$

$$d = eS + \epsilon E \tag{5}$$

In the above equation ‘c’ is elasticity vector, ‘E’ is the electric field, ‘S’ is strain vector, ‘e’ is dielectric, ‘d’ is electric displacement and matrix ‘ε’ is piezoelectric matrix. The resonant frequency of the sensor is expressed as equation 6.

$$F = V / \lambda \tag{6}$$

Where V is acoustic wave velocity and λ is wavelength of propagating wave [25].

Cylindrical CNTFET with constant thickness 1.5 nm and (at temperature 300 k) the distinct dielectric materials like teflon (2.1), silicon nitride (7), hafnium dioxide (15), zirconium dioxide (25), titanium dioxide (35) are considered and the brunt of these changes are studied for various specifications like drain induced barrier lowering (DIBL), transconductance (g<sub>m</sub>), output Conductance (g<sub>d</sub>), voltage gain (A<sub>v</sub>), subthreshold swing (SS).

The sensor is designed and simulated using COMSOL Multiphysics. The sensor is designed in 2 dimensional planes. The sensor uses a

piezoelectric substrate of 260µm length and 100 µm height which is constructed with lithium niobate (LiNbO3). Over this a sensing layer is placed with 260µm length and 20µm height. Here, a material used for sensing layer is TiO<sub>2</sub>. The performance of the sensor varies with the type of sensing layer used. The input and output IDT’s are constructed with 20µm of width and 200nm of height. The spacing between the IDT’s is 3µm. The material used for IDT’s is aluminium. The space between input and output IDT is called pitch which is in the order of 20µm. Besides the IDT’s air reflectors are constructed with 5 µm width and 10 µm height to reflect the air. The spacing between the air reflectors is 2µm [12]. The designed sensor is shown in Fig.1.

This sensor is designed and simulated in COMSOL Multiphysics using solid mechanics and electrostatics. The sensing layer properties like poisons ratio, relative permittivity and Young’s modulus are defined using parameters menu. In solid mechanics the properties of piezoelectric material are defined. Charge conversion over the surface of the sensor is defined in electrostatics.

The input and output IDT’s are applied with floating potential and ground potential alternatively. The air reflectors are filled with air. The periodic condition and fixed constraints defines the boundaries of the sensor. The performance of the sensor is studied using Eigen frequency and electric potential on the surface of the sensor. Fig. 2 shows the front view of sensor with coarse mesh analysis [12].

## RESULT AND DISCUSSIONS

The analysis of sensor is done using FEM using frequency dependent study. The displacement of

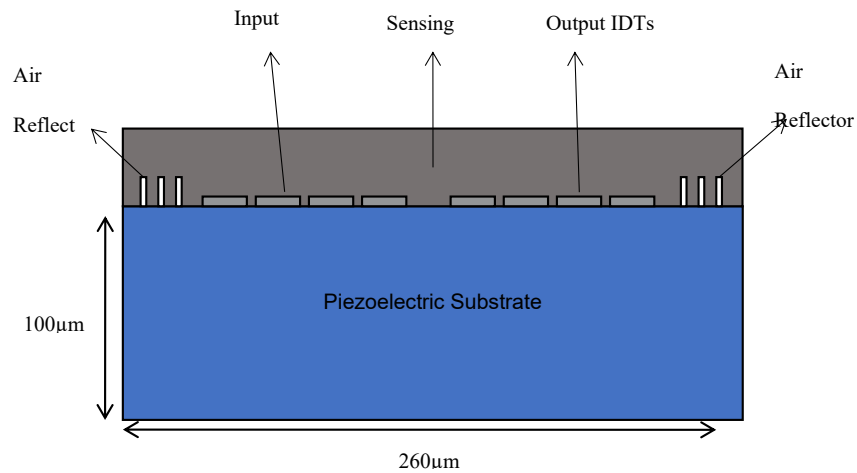


Fig. 1. The structure of designed SAW sensor.

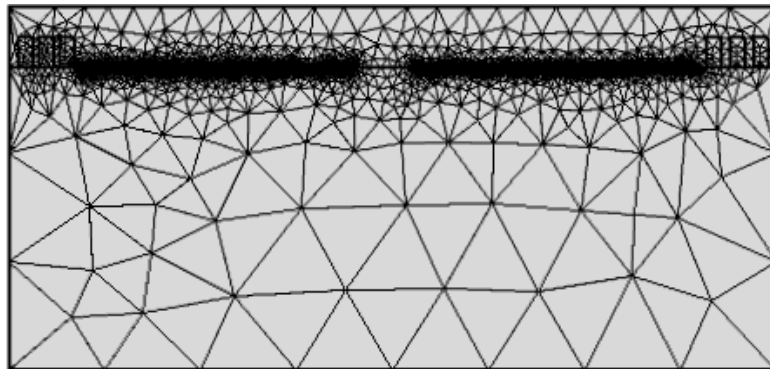


Fig. 2. Meshing view of constructed SAW sensor.

the sensor with respect to the change in frequency is studied. The performance of the sensor is evaluated by varying the concentration of hydrogen gas from 0.1ppm to 100ppm. Hydrogen is a gas which becomes reducing agent when mixed with non-metals and becomes oxidizing agent when mixed with metals. When the hydrogen gas gets imposed on the sensing layer the conductivity of the sensing layer varies which in turn changes the properties of the surface acoustic wave propagating on the surface of the sensor.

The performance of the sensor is observed by varying the concentration from 0.1ppm to 100ppm. The displacement of the sensor is increasing with increase in concentration. Using  $\text{TiO}_2$  nanomaterial the performance of the sensor is investigated with respect to the frequency. The operating frequency of the sensor is found to be 44 MHz. By considering  $\text{TiO}_2$  as the sensing layer, there exists an increment in the displacement of

the sensor for the same concentrations. Fig. 3 shows the change in displacement using  $\text{TiO}_2$  for when concentration is varied from 0.1 ppm to 100 ppm.

Fig. 4 shows the maximum displacement provided by the  $\text{TiO}_2$  sensing layer when the concentration is 100ppm. The performance of sensor is also studied by varying IDT height from  $0.05\mu\text{m}$  to  $0.5\mu\text{m}$  for  $\text{TiO}_2$  as a sensing layer. It is seen that, at the same IDT height and concentration  $\text{TiO}_2$  nano material gives better displacement than other sensing materials such as zinc oxide.

Fig. 5 shows the change in the displacement of  $\text{TiO}_2$  sensing layer with change in IDT height at 100ppm concentration. Apart from the effects of concentration, it is investigated that change in IDT height may result significantly in sensor responses. Thus the response increased with optimized IDT height. Fig. 6 shows the change in displacement with concentration for different

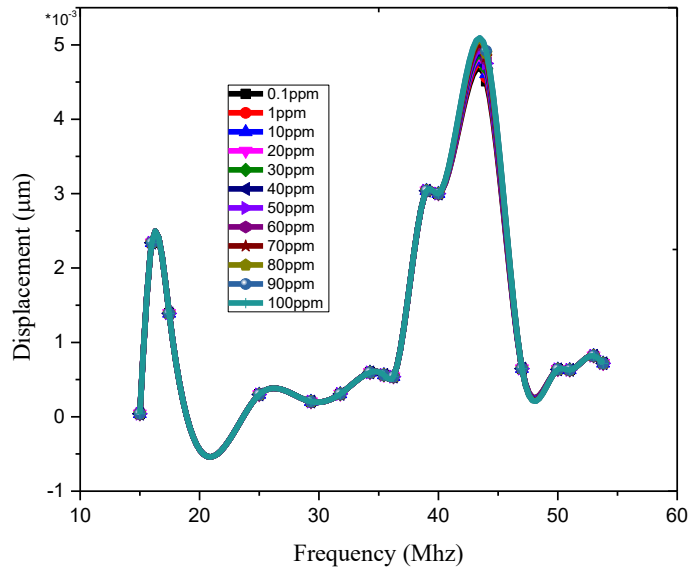


Fig. 3. Change in displacement of TiO<sub>2</sub> sensing layer for varying concentration.

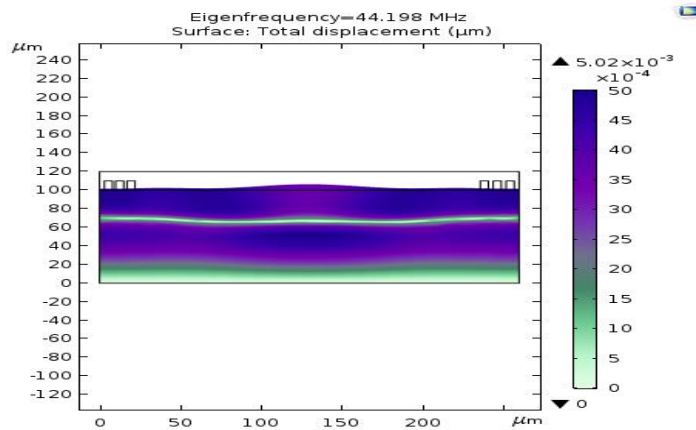


Fig. 4. Maximum displacement of TiO<sub>2</sub> sensing layer at 100ppm.

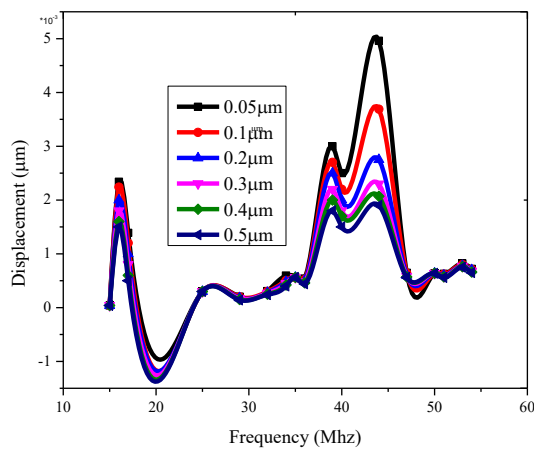


Fig. 5. Variation of displacement with varying IDT heights (from 0.05µm to 0.5µm) at 100ppm for TiO<sub>2</sub>.

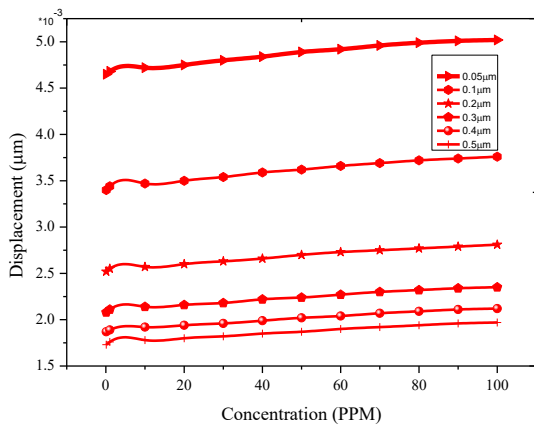


Fig. 6. Displacement verses concentration for different IDT heights.

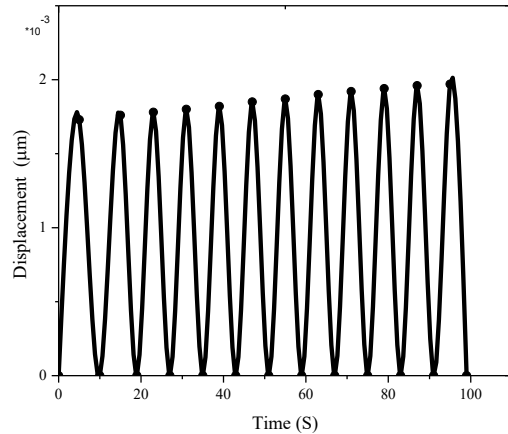


Fig. 7. Response time of the sensor.

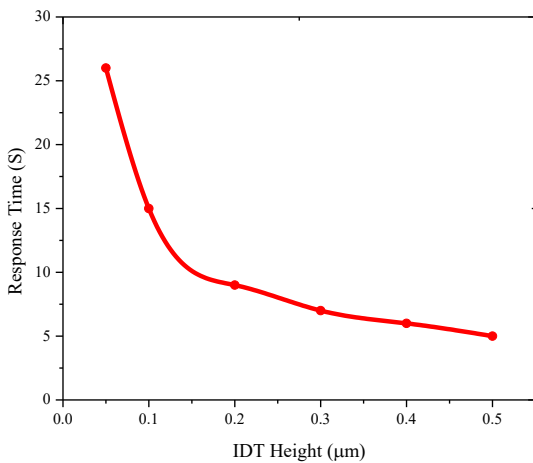


Fig. 8. Response time verses IDT height.

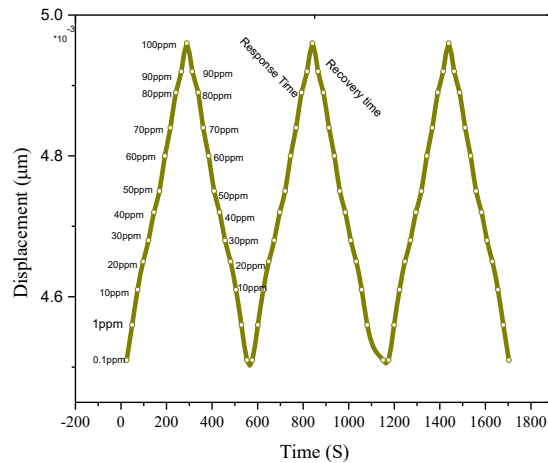


Fig. 9. Loading and unloading of sensor.

IDT heights. It is very clear that the displacement increases with increased target concentration as per the proposition. So from the plot it is clear that concentration plays major role in increment and decrement of the displacement and thus sensitivity. In the Fig. 5, red colour denotes the performance of TiO<sub>2</sub> nanomaterial.

The response time of sensor is also a key parameter to characterize the sensor. Response time is the time taken by the sensor to reach the final output stage from the present stage when input is applied. Fig. 7 shows the response time of the designed sensor. From the simulation it is observed that the response time of the sensor is varying with the IDT height. At IDT height of 0.05 µm the response time is same for both the nanomaterials and it slightly varied at other IDT heights. Fig.8 shows the change in response time

with IDT height. Fast response – recovery time is always appreciable for a sensor. An effective sensor is said to have zero hysteresis error, which indicates that the sensor output is same during loading and unloading. Fig. 9 indicates the zero hysteresis plot of designed sensor.

**CONCLUSION**

A nanostructured based SAW gas sensor is designed to detect different concentrations of hydrogen gas with high sensitivity. The sensor is simulated for concentrations ranging from 0.1 ppm to 100 ppm with ZnO and TiO<sub>2</sub> as sensing layers. Performance of the sensor is also observed for different IDT height for two nanomaterials. In simulation study, it is seen that the sensing performance of TiO<sub>2</sub> based SAW sensor enhances at same operating frequency of 44 MHz. The

sensor with IDT height 0.05  $\mu\text{m}$  and  $\text{TiO}_2$  as a sensing layer gives better results than other IDT heights and sensing materials. The future work includes introduction of an additional sensing layer to increase the performance of the multi layered sensor.

#### ACKNOWLEDGEMENTS

The author would like to acknowledge, Nanoelectronics lab, National MEMS Design Center, Sree Vidyanikethan Engineering College, Tirupati for providing the COMSOL Multiphysics for entire simulation work.

#### CONFLICT OF INTEREST

The authors declare that there is no conflict of interest.

#### REFERENCES

- [1] Awang Z., (2014), Gas sensors: A review. *Sens. Transducers*. 168: 61-75.
- [2] Anand M., (2005), Study of tin oxide for hydrogen gas sensor applications. *Thesis, University of South Florida, Graduate School*. 1- 98.
- [3] Arabshahi S., Dousti M., Hassan F. F., (2012), Simulation of surface acoustic wave  $\text{NO}_2$  gas sensor based on ZnO/XY  $\text{LiNbO}_3$  structure. *IJERA*. 2: 2120-2123.
- [4] Valluru S. P. R., (2015), Design of FIDT for 3D analysis of MEMS based gas sensor using SAW technology. *In Proceed. Comsol Conf.* in Pune.
- [5] Sarkar A., Venkataramana P., Harathi N., Jyothsna T., Teja N. V., (2020), Design and optimization of ZnO nanostructured SAW-based ethylene gas sensor with modified electrode orientation. *ASTES*. 5: 263-266.
- [6] Ippolito S. J., Ponzoni A., Kalantar-Zadeh K., Wlodarski W., Comini E., Faglia G., Sberveglieri G., (2006), Layered  $\text{WO}_3/\text{ZnO}/36^\circ \text{LiTaO}_3$  SAW gas sensor sensitive towards ethanol vapour and humidity. *Sens. Actuators B: Chem*. 117: 442-450.
- [7] Sarkar A., Maity S., Bhunia C. T., Sahu P. P., (2017), Responsivity optimization of methane gas sensor through the modification of hexagonal nanorod and reduction of defect states. *Superlatt. Microstruct.* 102: 459-469.
- [8] Powell S., David A., Kalantar-Zadeh K., Wlodarski W., Ippolito G., (2006), Layered surface acoustic wave chemical and bio-sensors. *Encyclop. Sens*. 5: 245-262.
- [9] Du Plessis H. G., Perold W. J., (2013), Simulation of ZnO Enhanced SAW Gas Sensor. *In Proceed. Comsol Conf.* in Rotterdam.
- [10] Kirschner J., (2010), Surface acoustic wave sensors (SAWS). *Micromechanical Syst*. 6: 1-11.
- [11] Ballantine Jr D. S., White R. M., Martin S. J., Ricco A. J., Zellers E. T., Frye G. C., Wohltjen H., (1996), Acoustic wave sensors: Theory, design and physico-chemical applications. Book: 1st Edition. *Elsevier*.
- [12] Harathi N., Kavitha S., Sarkar A., (2020), ZnO nanostructured 2D layered SAW based hydrogen gas sensor with enhanced sensitivity. *Mat. Today: Proceed.* (in Press).
- [13] Sarkar A., Maity S., Bhunia C. T., Sahu P. P., (2017), Responsivity optimization of methane gas sensor through the modification of hexagonal nanorod and reduction of defect states. *Superlatt. Microstruct.* 102: 459-469.
- [14] Sarkar A., Maity S., Joseph A. M., Chakraborty S. K., Thomas T., (2017), Methane-sensing performance enhancement in graphene oxide/Mg : ZnO heterostructure devices. *J. Electron. Mater.* 46: 5485-5491.
- [15] Hasan M. N., Maity S., Sarkar A., Bhunia C. T., Acharjee D., Joseph A. M., (2017), Simulation and fabrication of SAW-based gas sensor with modified surface state of active layer and electrode orientation for enhanced  $\text{H}_2$  gas sensing. *J. Electron. Mater.* 46: 679-686.
- [16] Zhao X., Wang L., Wang K., Lu G., (2007), Virtual operation of MEMS devices based on FEM simulation. In: *2007 2nd IEEE Int. Conf. Nano/Micro Eng. Molec. Sys. IEEE*. 122-126.
- [17] Shibayama K., Yamanouchi K., Sato H., Meguro T., (1976), Optimum cut for rotated Y-cut  $\text{LiNbO}_3$  crystal used as the substrate of acoustic-surface-wave filters. *Proceed. IEEE*. 64: 595-597.
- [18] Matatagui D., Kolokoltsev O., Saniger J. M., Gràcia I., Fernández M. J., Fontecha J. L., Horrillo M. D. C., (2017), Acoustic sensors based on amino-functionalized nanoparticles to detect volatile organic solvents. *Sens*. 17: 2624-2629.
- [19] Wang S. H., Kuo S. H., Shen C. Y., (2011), A nitric oxide gas sensor based on Rayleigh surface acoustic wave resonator for room temperature operation. *Sens. Actuators B: Chem*. 156: 668-672.
- [20] Hao H. C., Lin T. H., Chen M. C., Yao D. J., (2010), January. A chemical surface acoustic wave (SAW) sensor array for sensing different concentration of  $\text{NH}_3$ . In : *IEEE 5th Int. Conf. Nano/Micro Eng. Molec. Sys. IEEE*. 1092-1096.
- [21] Tsai H. H., Wu D. H., Chiang T. L., Chen H. H., (2009), Robust design of saw gas sensors by taguchi dynamic method. 9: 1394-1408.
- [22] Zhao X., Wang L., Wang K., Lu G., (2007), Virtual operation of MEMS devices based on FEM simulation. In : *2nd IEEE Int. Conf. Nano/Micro Eng. Molec. Sys. IEEE*. 122-126.
- [23] Maouhoub S., Aoura Y., Mir A. J. M. E., (2015), FEM simulation of rayleigh waves for SAW devices based on ZnO/AlN/Si. *Microelec. Eng*. 136: 22-25.
- [24] Ippolito S. J., Kalantar-Zadeh K., Wlodarski W., Powell D., (2002), Finite-element analysis for simulation of layered SAW devices with XY  $\text{LiNbO}_3$  substrate. In: *Smart Structures, Devices, and Systems*. In Conference Proceedings of SPIE. *Int. Soc. Opt. Eng.* 120-131.
- [25] Water W., Chen S. E., (2009), Using ZnO nanorods to enhance sensitivity of liquid sensor. *Sens. Actuators B: Chem*. 136: 371-375.
- [26] Abbasi A., Jahanbin Sardroodi J., (2016), A theoretical study on the adsorption behaviors of Ammonia molecule on N-doped  $\text{TiO}_2$  anatase nanoparticles: Applications to gas sensor devices. *Int. J. Nano Dimens*. 7: 349-359.